

SIMULATION AND THEORY OF THE IMPACT OF TWO-DIMENSIONAL ELASTIC DISKS

Hisao Hayakawa^{*}, Hiroto Kuninaka

*Graduate School of Human and Environmental Studies, Kyoto University,
Sakyo-ku, Kyoto, 606-8501, Japan*

Abstract

The impact of a two-dimensional elastic disk with a wall is numerically studied. It is clarified that the coefficient of restitution (COR) decreases with the impact velocity. The result is not consistent with the recent quasi-static theory of inelastic collisions even for very slow impact. This suggests that the elastic model cannot be used in the quasi-static limit. A new quasi-static theory of impacts is proposed, in which the effect of thermal diffusion is dominant. The abrupt decrease of COR has been found due to the plastic deformation of the disk, which is assisted by the initial internal motion.

Key words: Dynamic simulation, Elasticity, Granular, Heat conduction, Kinetics, Numerical Analysis

^{*} Corresponding author. Tel.: +81-75-753-6782; fax: +81-75-753-2931.
Email address: hisao@yuragi.jinkan.kyoto-u.ac.jp (Hisao Hayakawa).

1 Introduction

The collision of particles with the internal degrees of freedom is inelastic in general. The inelastic collisions are abundant in nature (Goldsmith, 1960). Examples can be seen in collisions of atoms, molecules, elastic materials, balls in sports, and so on. The study of inelastic collisions will be able to be widely accepted as one of fundamental subjects in physics, because they are almost always discussed in textbooks of elementary classical mechanics.

Physicists realize that inelastic collisions can be a fashionable subject in physics from recent extensive interest in granular materials (Kadanoff, 1999; de Gennes, 1999). In fact, granules consist of macroscopic dissipative particles. Therefore, the decision of interaction among particles is obviously important. We believe that static interactions among granular particles can be described by the theory of elasticity (Love, 1927; Landau et al., 1960; Johnson, 1985; Hills et al., 1993). For example, the normal compression may be described by the Hertzian contact force (Hertz, 1882) and the shear force may be represented by the Mindlin force (Mindlin, 1949). The dynamical part related to the dissipation, however, cannot be described by any reliable physical theory. Thus, the distinct element method (Cundall & Struck, 1979) which is one of the most popular models to simulate collections of granular particles contains some dynamical undetermined parameters. In other words, to determine such the parameters is important for both granular physics and fundamental physics.

The normal impact of macroscopic materials is characterized by the coefficient of restitution (COR) defined by

$$e = -v_r/v_i, \tag{1}$$

where v_i and v_r are the relative velocities of incoming and outgoing particles respectively. COR e had been believed to be a material constant, since the classical experiment by Newton (1662). In general, however, experiments show that COR for three dimensional materials is not a constant even in approximate sense but depends strongly on the impact velocity (Goldsmith, 1960; Sondergaard et al., 1990; Bridges et al., 1984; Supulver et al., 1995; Giese et al., 1996; Aspelmeier et al., 1998; Basile et al., 2000; Labous et al., 1995).

The origin of the dissipation in inelastic collisions is the transfer of the kinetic energy of the center of mass into the internal degrees of freedom during the impacts. Systematic theoretical investigations of the impact have begun with the paper by Kuwabara and Kono (1987). Taking into account the viscous motion among the internal degrees of freedom, they derived the equation of the macroscopic deformation. Later, Brilliantov *et al.* (1996) and Morgado and Oppenheim (1997) derived the identical equation to eq.(2). In particular, the derivation by Morgado and Oppenheim (1997) is based on the standard technique of nonequilibrium statistical mechanics to extract the slow mode among the fast many modes which can be regarded as the thermal reservoir with constant temperature (see Appendix). Furthermore, Brilliantov *et al.* (1996) compared their theoretical results with experimental results. Thus, the quasi-static theory has been accepted as reasonable one.

On the other hand, Gerl and Zippelius (1999) performed the microscopic simulation of the two-dimensional collision of an isothermal elastic disk with a wall. Their simulation is mainly based on the mode expansion of an elastic disk under the force free boundary condition. The distinct characteristic of their model is that they do not introduce any dissipative mechanism of their microscopic equation of motion. Then, they solve Hamilton's equation deter-

mined by the elastic field and the repulsive potential to represent the collision of two disks. Their results show that COR decreases with the impact velocity, which strongly depends on Poisson's ratio. For high velocity of the impact they demonstrate the macroscopic deformation left after the collision is over. The relation between the quasi-static theory of impact (Kuwabara & Kono, 1987; Brilliantov et al., 1996; Morgado & Oppenheim, 1997) and their microscopic simulation (Gerl & Zippelius, 1999) is not trivial, because the energy transfer during the impact is not explicitly included in the quasi-static theory. Thus, we have to clarify the relation between two typical approaches.

In this paper, we will perform the microscopic simulation of the impact of a two dimensional elastic disk with a wall. We introduce two methods of simulation: one is based on the lattice model (model A) and another is a continuum model (model B) which is identical to that by Gerl and Zippelius (1999). Both models do not include any dissipation explicitly. Thus, we regard inelastic collisions take place only from the transfer of modes of oscillation. Through our simulation, we will demonstrate that the elastic models do not recover the results predicted by the quasi-static theories in the low impact velocity (Kuwabara & Kono 1987; Brilliantov et al., 1996; Morgado & Oppenheim, 1997; Schwager et al., 1998; Ramírez et al., 1999).

The organization of this paper is as follows. In the next section, we will briefly review the outline of quasi-static theory (Kuwabara & Kono, 1987; Brilliantov et al., 1996; Morgado et al., 1997). In section 3, we will explain model A and model B which is equivalent to the model by Gerl and Zippelius (1999) of our simulation. In section 4, we will show the result of our simulation and discuss the validity of quasi-static theory. In section 5, we will discuss our results. In section 6, we will summarize our result. In Appendix, we summarize the

outline of the quasi-static theory by Morgado and Oppenheim (1997). Note that parts of this paper has been published as separated papers (Hayakawa & Kuninaka.,2001a; Hayakawa & Kuninaka, 2001b; Kuninaka & Hayakawa, 2001).

2 Quasi-Static Theory: Review

In this section, we briefly explain the outline of the quasi-static theory. One purpose of this section is to summarize the two-dimensional version of quasi-static theory which may not be mentioned in any articles explicitly.

At first, let us summarize the three dimensional result, in which the equation of the macroscopic deformation is given by

$$\ddot{h} = -k_h(h^{3/2} + A_h\sqrt{h}\dot{h}) \quad (2)$$

in a collision of two spheres. For the collision of two identical spheres the macroscopic deformation h is given by $h = 2R - |\mathbf{r}_1 - \mathbf{r}_2|$ with the radius R and the position of the center of the mass \mathbf{r}_i of i th particle. \dot{h} and \ddot{h} are respectively dh/dt and d^2h/dt^2 . k_h in eq.(2) is written as

$$k_h = \frac{\sqrt{2RY_0}}{3(1 - \sigma^2)M_0} \quad (3)$$

where M_0 , Y_0 and σ are the mass of the sphere, (three dimensional) Young's modulus, and Poisson's ratio, respectively. In eq.(2) A_h is a constant, which may be a function of viscous parameters (Brilliantov et al., 1996). The first term of the right hand side in eq.(2) represents the Hertzian contact force (Love, 1927; Landau et al., 1960; Johnson, 1985; Hertz, 1882) and the second

term is the dissipation due to the internal motion.

The simplest derivation of eq.(2) is that by Brilliantov *et al.* (1986), though we also check its validity by the alternative methods. Taking into account the limitation of the length of this paper, we follow the argument by them. The outline of the derivation by Morgado and Oppenheim (1997) is shown in Appendix.

The static stress tensor in a two-dimensional linear elastic material can be represented by

$$\sigma^{(el)}_{ij} = 2\mu(u_{ij} - \delta_{ij}u_{ll}/2) + K\delta_{ij}u_{ll} \quad (4)$$

where μ and K are respectively the shear modulus and the bulk modulus, and u_{ij} is given by

$$u_{ij} = \frac{1}{2} \left(\frac{\partial u_i}{\partial x_j} + \frac{\partial u_j}{\partial x_i} \right) \quad (5)$$

with the displacement field u_i .

The two dimensional Hertzian contact law (Johnson, 1985; Gerl et al., 1999) is given by the relation between the macroscopic deformation of the center of mass h and the elastic force F_{el} as

$$h \simeq -\frac{F_{el}}{\pi Y} \left\{ \ln \left(\frac{4\pi Y R}{F_{el} (1 - \sigma^2)} \right) - 1 - \sigma \right\}, \quad (6)$$

where Y is (two-dimensional) Young's modulus. Note that F_{el} and Y do not have dimension of the force and Young's modulus, because these are two dimensional variables which are the ones per unit length along the third axis. Equation (6) can be derived from the stress tensor (4) with the standard treat-

ment of linear elastic theory. Note that h satisfies $h = R - y_0$ with the position of the center of mass y_0 (Gerl & Zippelius, 1999).

For small dissipation, as in Landau & Lifshitz (1960), the dissipative stress tensor due to the viscous motion among internal motions is given by

$$\sigma^{(vis)}_{ij} = 2\eta_1(\dot{u}_{ij} - \delta_{ij}\dot{u}_{ll}/2) + \eta_2\delta_{ij}\dot{u}_{ll}, \quad (7)$$

where \dot{u}_{ij} is the time derivative of u_{ij} , η_i ($i = 1, 2$) is the viscous constant.

Brilliantov *et al.* (1996) assumed that the velocity of deformation field is governed by the macroscopic deformation, *i.e.*, $\dot{u}_i \simeq \dot{h}(\partial u_i / \partial h)$. Since in the limit of $v_i \rightarrow 0$ we may replace eq.(6) by $F_{el} \simeq -\pi Y h / \ln(4R/h)$ (Gerl & Zippelius, 1999). Thus, with the aid of the assumption by Brilliantov *et al.* (1996), (4) and (7), it is easy to derive the two dimensional version of quasi-static theory as

$$F_{tot} \simeq -\frac{\pi Y h}{\ln(4R/h)} - A \frac{\pi Y \dot{h}}{\ln(4R/h)}, \quad (8)$$

where A is not an important constant. This result can be derived by various other methods. In section 4, we will compare the result of our simulation with eq.(8).

3 Our Models

Let us explain the details of our models to simulate collisions between two identical disks whose radius R by the method of the mirror image. In both models, the wall exists at $y = 0$, and the center of mass of the disk keeps

the position at $x = 0$. The disk approaches from the region $y > 0$ before rebounding from the wall.

3.1 Model A

The disk in model A consists of some mass points (with the mass m) on a triangular lattice. All the mass points are connected with linear springs with spring constant κ . In the limit of a large number of mass points, this disk corresponds to the continuum circular disk with Young's modulus $Y = 2\kappa/\sqrt{3}$ and Poisson's ratio $1/3$ (Hoover, 1991). The position of each mass point of model A is governed by the following equation:

$$m \frac{d^2 \mathbf{r}_p}{dt^2} = -\kappa \sum_{i=1}^6 (d_0 - |\mathbf{r}_p - \mathbf{r}_i|) \frac{\mathbf{r}_p - \mathbf{r}_i}{|\mathbf{r}_p - \mathbf{r}_i|} + \mathbf{e}_y a_0 V_0 e^{-a_0 y_p} \quad (9)$$

where d_0 is the lattice constant, \mathbf{r}_i is the position of the nearest neighbor mass points of \mathbf{r}_p , m is the mass of the mass points, y_p is the y coordinate of \mathbf{r}_p , and \mathbf{e}_y is the unit vector in the y direction. Note that the directional projection of the linear spring force in model A can cause the nonlinear deformation. The wall potential is given by $V_0 e^{-a_0 y}$, where $V_0 = mc^2 a_0 d_0 / 2$ with $c = \sqrt{Y/\rho}$ and the density ρ . We adopt $a_0 = 100/d_0$ for the most of simulations, but we also adopt the result of $a_0 = 25/d_0 = 500/R$ to obtain Fig.2, though the result is almost identical to that for $a = 100/d_0$. The exponential interaction between the disk and the wall is introduced to simulate a collision between two identical disks. Actually, in the limit of $a_0 \rightarrow \infty$, the exponential potential can be regarded as a potential of the mirror image. Thus, for later calculation, we analyze the case for large $a_0 d_0$. The number of mass points is fixed at 1459 in model A, since the rough evaluation of convergence of the results has been

checked in this model.

3.2 Model B

In this subsection, we introduce model B which is originally proposed by Gerl and Zippelius (1999). Although the details of this model can be found in their paper, we present a short description of this model to understand the setup of our simulation.

Gerl and Zippelius (1999) analyze Hamilton's equation to simulate collisions of a disk with the radius R as;

$$\dot{P}_{n,l} = -\frac{\partial H}{\partial Q_{n,l}}; \quad \dot{Q}_{n,l} = \frac{\partial H}{\partial P_{n,l}} \quad (10)$$

under the Hamiltonian

$$H = \frac{P_0^2}{2M} + \sum_{n,l} \left(\frac{P_{n,l}^2}{2M} + \frac{1}{2} M \omega_{n,l}^2 Q_{n,l}^2 \right) + V_1 \int_{-\pi/2}^{\pi/2} d\phi e^{-a_0 y(\phi,t)}. \quad (11)$$

Here M is the (two-dimensional) mass of an elastic disk, and $Q_{n,l}$ is the expansion coefficient of the 2D elastic deformation field in the polar coordinate

$$\mathbf{u} = (u_r, u_\phi)$$

$$(u_r(r, \phi), u_\phi(r, \phi)) = \sum_{n,l} Q_{n,l} (u_r^{n,l}(r) \cos n\phi, u_\phi^{n,l}(r) \sin n\phi), \quad (12)$$

where $u_r^{n,l}(r)R = A_{n,l} \frac{dJ_n(k_{n,l}r)}{dr} + nB_{n,l} \frac{J_n(k'_{n,l}r)}{r}$ and $u_\phi^{n,l}(r)R = -nA_{n,l} \frac{J_n(k'_{n,l}r)}{r} - B_{n,l} \frac{dJ_n(k_{n,l}r)}{dr}$ with the radius of the disk and the Bessel function of the n -th order $J_n(x)$. Here $k'_{n,l} = k_{n,l} \sqrt{2(1+\sigma)/(1-\sigma^2)}$ and $k_{n,l}$ is the solution of

$$(1-\sigma^2)(1-n^2)\kappa\kappa'^2 J_{n-1}(\kappa)J_{n-1}(\kappa') + \kappa^2[\kappa^2 - 2n(n+1)(1-\sigma)]J_n(\kappa)J_n(\kappa')$$

$$+(1 - \sigma)[\kappa^2 - (1 - \sigma)(1 - n^2)n][\kappa J_{n-1}(\kappa)J_n(\kappa') + \kappa' J_{n-1}(\kappa')J_n(\kappa)] = 0 \quad (13)$$

with Poisson's ratio σ , $\kappa = k_{n,l}R$ and $\kappa' = k'_{n,l}R$, which is given by the force free boundary condition of the disk:

$$\sigma_{r\phi}(R, \phi) = 0 \quad (14)$$

Thus, for fixed n there are infinitely many solutions $k_{n,l}$ and $\omega_{n,l} = k_{n,l}\sqrt{Y/\{\rho(1 - \sigma^2)\}}$ numbered by $l = 0, 1, \dots, \infty$. $A_{n,l}$ and $B_{n,l}$ are determined by

$$\begin{aligned} & -A_n \left[\frac{(1 - \sigma)}{R} \frac{dJ_n(k_{n,l}R)}{dR} + \left(k_{n,l}^2 - \frac{(1 - \sigma)}{R^2} n^2 \right) J_n(k_{n,l}R) \right] \\ & + nB_n(1 - \sigma) \left[\frac{1}{R} \frac{dJ_n(k'_{n,l}R)}{dR} - \frac{J_n(k'_{n,l}R)}{R^2} \right] = 0 \end{aligned} \quad (15)$$

and $\int_0^R dr r \{u_r^{n,l^2} + u_\phi^{n,l^2}\} = R^2$. $P_{n,l}$ is the canonical momentum. $y(\phi, t)$ is the shape of the elastic disk in polar coordinates;

$$y(\phi, t) = y_0(t) + \sum_{n,l} Q_{n,l} (C_{n,l} \cos(n\phi) \cos \phi - S_{n,l} \sin(n\phi) \sin \phi) \quad (16)$$

with the position of the center of mass $y_0(t)$ and constants $C_{n,l}$ and $S_{n,l}$ determined by the maximal radial and tangential displacement at the edge of the disk as $C_{n,l} = u_r^{n,l}(R)$ and $S_{n,l} = u_\phi^{n,l}(R)$. M is the mass of the disk, and the momentum of the center of the mass $P_0 = My_0$ satisfies $\dot{P}_0 = -(\partial H/\partial y_0)$, V_0 and a are parameters to express the strength of the wall potential.

For the simulation of a pair of identical disks, they have confirmed that the result with finite a_0 can be extrapolated to the result of $a_0 \rightarrow \infty$ by taking into account finite a_0 effect in proportion to $1/(a_0R)$. Similarly, the result with finite number of modes N should be extrapolated with the correction in proportion to $1/\sqrt{N}$. Since they have already checked such the tendencies, we

only adopt $N = 1189$ ($n \leq 50$ and $\kappa_n \leq 50$) or $N = 437$ ($n \leq 30$ and $\kappa_n \leq 30$), $V_1 = Mc^2 a_0 R/2$ and $a_0 = 500/R$.

3.3 Parameters in both models

For the comparison between two different models, we only simulate the case of Poisson's ratio $\sigma = 1/3$. The numerical integration scheme for model A is the classical fourth order Runge-Kutta method with $\Delta t = 1.6 \times 10^{-3} \sqrt{m/\kappa}$. Parts of the calculation in model A has been checked by the fourth order symplectic integral method with $\Delta t = 5.0 \times 10^{-3} \sqrt{m/\kappa}$, and no differences in results of two methods can be found. For model B, we adopt the fourth order symplectic integral method with $\Delta t = 5.0 \times 10^{-3} R/c$. In both models, we have checked for conservation of the total energy.

We also investigate the impact with finite temperature. The temperature is introduced as follows: In model A, we prepare the Maxwellian for the initial velocity distribution of mass points, where the positions of all mass points are located at their equilibrium positions. From the variance of the Maxwellian we can introduce the temperature as a parameter. To perform the simulation, we prepare 10 independent samples obeying Maxwellian with the aid of normal random number. In model B, we prepare samples which satisfies Gibbs states. Namely, $\sqrt{M}\omega_{n,l}Q_{n,l}/\sqrt{2}$ and $P_{n,l}/\sqrt{2M}$ obey the normal random number with the variance (temperature) T . In model B, we prepare many samples (120 or 20) to simulate systems at finite T .

The summary of differences between model A and B is as follows: (i) All of the mass points in model A interact with the wall but, in model B, only the

exterior boundary has the influence of the potential as in eq.(11). We have replaced the original model A by a model in which only mass points on the boundary can interact with the wall, but we cannot find significant differences in the results of our simulation in both discrete models. (ii) Model A can have nonlinear deformations, but model B is based on the theory of linear elasticity. (iii) Model A can express some plastic deformations, but model B cannot. This effect will be discussed in section 6. (iv) Model A has six fold symmetry whereas model B has only rotational symmetry. (v) The force free boundary condition (14) is assumed in model B but may not be appropriate for actual situations. Model A does not include such the condition.

4 Results

Now, let us explain the details of the result of our simulation. In the first subsection, we will introduce the result at $T = 0$ and in the second subsection, we will show the result at finite T .

4.1 Simulation at $T = 0$

At first, we carry out the simulation of model A and model B with the initial condition at $T = 0$ (*i.e.* no internal motion). Figure 2 is the plot of the COR against the impact velocity for both model A and model B. For model A, we have adopted the fourth order Runge-Kutta method. To eliminate the effect of six fold symmetry of model A, we average 12 data as a function θ of the initial orientations of the disk *i.e.* $\theta = \pi n/72$ with $n = 1, 2, 3, \dots, 12$ with $a_0 = 25/d_0 = 500/R$ for $N = 1459$. We also investigate the case that only

mass points at the boundary can interact with the wall for small v_i but their results do not have any visible difference from the original model A. It is obvious that there is no plastic deformations for $v_i \leq 0.2c$.

For model B, we show the results of 437 modes and 1189 modes which clearly demonstrates the convergence of the result for the number of modes. When impact velocity v_i is larger than $0.1c$ with $c = \sqrt{Y/\rho}$, the value of COR of model A is almost identical to that of model B. Each line decreases smoothly as impact velocity increases.

At present, we do not know the reason why the significant difference between the two models exists at low impact velocity. It is difficult to imagine that occurrence of nonlinear deformations during the impact of model A causes the difference because the deformation is smaller when v_i is smaller.

Second, we investigate the force acting on the center of mass of the disk caused by the interaction with the wall in model B. In the limit of $v_i \rightarrow 0$ we expect that the Hertzian contact theory can be used (Landau & Lifshitz, 1960; Johnson, 1985; Gerl & Zippelius, 1999). The small amount of transfer from the translational motion to the internal motion is the macroscopic dissipation. Thus, we can check whether the quasi-static approaches (Kuwabara & Kono, 1987; Brilliantov et al., 1996; Morgado & Oppenheim, 1997) or our elastic simulation can be used in slow impact situations.

If h is given, we can calculate the elastic force by solving eq.(6) numerically. Figure 3 is the comparison with our simulation in model B (1189 modes) and the Hertzian contact theory (6) which is given by the solid lines. The result of our simulation at the impact velocity $v_i = 0.01c$ shows the hysteresis as suggested in the simulation at $v_i = 0.1c$ (Gerl & Zippelius, 1999). This means

the compression and rebound are not symmetric. The hysteresis curve is still self-similar even at $v_i = 0.04c$ but the loop becomes noisy at $v_i = 0.1c$.

For very low impact velocity $v_i = 0.001c$, the hysteresis loop almost disappears and the total force observed in our simulation is almost a linear function of h which deviates from the one predicted by both the Hertzian contact theory and the quasi-static theory (8). In particular, the turning point which corresponds to the point of the largest F_{tot} in Fig. 3(b) is apart from the Hertzian curve (the solid line). This deviation is in clear contrast to the quasi static theory, because the dissipative force in the theory in eqs.(2) and (8) must be zero at the turning point which $\dot{h} = 0$ should satisfy. This tendency is invariant even for the simulation of model A, though the data becomes noisy. The linearity of the total repulsion force is not surprising, because $e^{-a_0 y(\phi, t)}$ in the potential term in eq.(11) can be expanded in a series of $Q_{n,l}$ for very slow impact.

The result may suggest that our elastic models do not recover the Hertzian contact theory in the quasi-static limit. To check the tendency, we investigate whether any static state can be achieved in our models in the compression. Figure 4 is the time evolution of the center of mass in the simulation of model B, where the strength of dimensionless external field is $g = 0.01c^2/R$. We observe that an undamped harmonic oscillation of the center of mass in the simulation after the first deformation. This oscillation is stable because the energy of oscillation is not enough to overcome finite energy gap between energy levels. Thus, the center of mass keeps the oscillation as the motion in the ground state. We note that Fig.4 is the result of the simulation at finite temperature in which the mode transfer is enhanced. Nevertheless, the center of mass keeps the harmonic oscillation. This tendency can be observed in model A, too. Even when we introduce the randomness in the coupling

in model A, the oscillation is undamped. Thus, both of elastic models cannot reach any equilibrium steady state as is assumed in the Hertzian contact theory. This result indicates that the elastic models are not appropriate to describe quasi-static situations for $v_i/c \ll 1$. Note that the introduction of nonlinear deformation may not be enough, because as we can see in Fig.3 (b) the deformation is very small for slow impact. Thus, it is difficult to imagine the impact produces nonlinear deformations. To reach an equilibrium state, thus, we need to introduce some microscopic dissipative mechanism.

However, the validity of the contact time τ in the impact evaluated as $\tau \simeq (\pi R/c)\sqrt{\ln(4c/v_i)}$ by the quasi-static theory (Gerl & Zippelius, 1999) has been confirmed by the results of our simulation of model A (Fig.5). Thus, our elastic model can be valid in the impact with the intermediate speed.

4.2 Simulation at finite T

Now, let us show the results of our simulation at finite T . The thermal velocity $v_{th} = \sqrt{T/M}$ causes significant differences from those at $T = 0$ in both low and large impact velocities. In this sense, we have much room to study this process at finite T systematically.

For small impact velocity, i.e. if the effect of v_{th} is not negligible, the fluctuation of COR at finite T becomes large, while the average is almost independent of temperature as in Figs. 6 and 7, where the results are obtained from the average of 120 independent samples. In some trials at high temperature, thus, COR becomes larger than 1, though the average is less than 1. Of course, for such the high temperature, it is impossible to control the actual speed of

impact.

For large impact velocity, $v_i \gg v_{th}$, we do not observe any definite temperature effect in model B but we find drastic decrease of COR in model A. It seems that COR can be on a universal curve when the impact velocity is scaled by the critical velocity above which the COR decreases abruptly (Fig.8). The relation between the critical velocity and the initial temperature at the intermediate impact velocities is shown in Fig. 9. The critical velocity seems to obey a linear function of T , though the data is not on the function for both slow and fast impacts.

5 Alternative Quasi-Static Theory: The Effect of Temperature Gradient

In this section, let us discuss new aspects of the quasi-static theory. As in section 2, the conventional quasi-static theories (Kuwabara & Kono, 1987; Brilliantov et al., 1996) consider the effect of internal friction. Similarly, the Langevin approach (Morgado & Oppenheim, 1997) gives the identical result to that by conventional one. In both approaches, it is assumed that the temperature in disks is uniform. However, this assumption is not accurate. It is known that the rise of temperature is proportional to the divergence of elastic deformation (Landau & Lifshitz, 1960). Thus, the temperature cannot be uniform.

In this section, we will evaluate the dissipation rate due to the thermal diffusion and show that the contribution of this term is dominant in quasi-static situations. The result may not be complete but meaningful to indicate the

importance of the thermal diffusion.

In a quasi-static collision, the compression is proceeded in an adiabatic process. The adiabatic condition is written as $S_0(T) + K\alpha u_{ii} = S_0(T_0)$, where S_0 , K , α and T_0 are respectively the entropy (divided by the Boltzmann constant), the bulk modulus, the thermal expansion rate and the temperature without any deformation (Landau, 1960). From the expansion of the entropy around T_0 we obtain

$$T - T_0 = -\frac{T_0 K_{ad} \alpha}{C_p} u_{ii} = -\frac{T_0 \alpha \rho}{C_p} (c_l^2 - c_t^2) u_{ii}, \quad (17)$$

where K_{ad} , C_p , c_l and c_t are the bulk modulus in the adiabatic process, the heat capacity at constant pressure, the sound velocity of the longitudinal mode and the sound velocity of the tangential mode, respectively (Landau & Lifshitz, 1960). To obtain the final expression we use the two-dimensional relations $K_{ad} = Y/(2(1 - \sigma))$, $c_l = \sqrt{Y/(\rho(1 - \sigma^2))}$ and $c_t = \sqrt{Y/(2\rho(1 + \sigma))}$. There is the relation between the stress tensor and the divergence of deformation u_{ii} as

$$u_{ii} = \frac{1 - \sigma}{Y} \sigma_{ii} = \frac{1 - \sigma}{Y} (\sigma_{xx} + \sigma_{yy}) \quad (18)$$

in the two-dimensional elastic medium (Landau & Lifshitz, 1960). Substituting (18) into (17) we obtain

$$T - T_0 = \frac{T_0 \alpha}{2C_p} \sigma_{ii}. \quad (19)$$

Thus, if σ_{ii} is a function of the position, the temperature field is not uniform, which is contrast to the assumption in previous quasi-static theory.

It is known that the thermal diffusion causes energy dissipation. The dissipa-

tion rate is given by

$$\dot{E} = -\frac{\kappa_T}{T_0} \int d^2\mathbf{r} (\nabla T)^2, \quad (20)$$

where κ_T is the thermal conductivity (Landau & Lifshitz, 1960). The integration in (20) is performed in all region of elastic disks. Thus, from (19) and (20), the energy dissipation which is not included in previous treatments is need to be considered.

Now, let us evaluate the integral (20). For this purpose, we use the exact solution of two-dimensional Hertzian contact problem (Hills et al., 1993). The explicit stress tensor is given by

$$\begin{aligned} \sigma_{xx} &= p_0 y \left[2 - \frac{s}{\sqrt{1+s^2}} - \frac{\sqrt{1+s^2}}{s} - \frac{\hat{x}^2 s^3}{(1+s^2)^{3/2}(s^4 + \hat{y}^2)} \right], \\ \sigma_{yy} &= -p_0 \frac{\hat{y}^3 \sqrt{1+s^2}}{s(s^4 + \hat{y}^2)}, \end{aligned} \quad (21)$$

where $\hat{x} = x/a$ and $\hat{y} = y/a$ are scaled by the contact radius a which is given by

$$a^2 = \frac{4F_{el}R(1-\sigma^2)}{Y} \quad (22)$$

for the contact of two identical disks. Note that x and y are the position in the Cartesian coordinate whose origin is the center of the contact area (see Fig. 10). p_0 in (21) is given by

$$p_0 = \frac{2F_{el}}{\pi a}, \quad (23)$$

where s in (21) is

$$s^2 = \frac{1}{2} \left\{ -(1 - \hat{x}^2 - \hat{y}^2) + \sqrt{(1 - \hat{x}^2 - \hat{y}^2)^2 + 4\hat{y}^2} \right\}. \quad (24)$$

From (21) we obtain σ_{ii}

$$\sigma_{ii} = p_0 \left\{ 2 - \frac{s}{\sqrt{1+s^2}} - \frac{s^3 \hat{x}^2}{(1+s^2)^{3/2}(s^4 + \hat{y}^2)} - \frac{\sqrt{1+s^2}(s^4 + 2\hat{y}^2)}{s(s^4 + \hat{y}^2)} \right\}, \quad (25)$$

Thus, the dissipation rate (20) can be calculated in principle.

Note that the numerical integration of (20) is not easy, because (i) the explicit expression is too complicated, (ii) the boundary is modified by the compression, and (iii) the parameter $\hat{R} \equiv R/a$ is important and is a function of the impact velocity. Thus, here, we present a rough analytical evaluation of (20) to capture the characteristics of this problem. We note that σ_{ii} becomes simple in some special situations. For example, σ_{ii} at $x = 0$ which is on the axis of symmetry is given by (Hills et al., 1993)

$$\sigma_{ii}^{in} \equiv \sigma_{ii}(0, \hat{y}) = 2p_0 \left[\hat{y} - \sqrt{1 + \hat{y}^2} \right]. \quad (26)$$

On the other hand, the integral representation of σ_{ii}

$$\sigma_{ii} = -\frac{2yp_0}{\pi} \int_{-a}^a d\xi \frac{\sqrt{a^2 - \xi^2}}{(x - \xi)^2 + y^2}, \quad (27)$$

can be approximated by

$$\sigma_{ii}^{out} \simeq -\frac{2yp_0}{\pi r^2} \int_{-a}^a d\xi \sqrt{a^2 - \xi^2} = -\frac{\hat{y}p_0}{\hat{r}^2} \quad (28)$$

far from $x = 0$. Here we use $\int_{-a}^a d\xi \sqrt{a^2 - \xi^2} = \pi a^2/2$.

For the evaluation of (20), we distinguish the inner part $|x| < a$ from the outer part $|x| > a$. In the inner region, we may replace σ_{ii} by σ_{ii}^{in} . Thus, $(\nabla T)^2$ in

the inner region may be approximated by

$$(\nabla T)_{in}^2 \simeq \frac{T_0^2 \alpha^2 p_0^2}{4C_p^2 a^2} \left(1 - \frac{\hat{y}}{\sqrt{1 + \hat{y}^2}}\right)^2. \quad (29)$$

In the outer region we may replace σ_{ii} by σ_{ii}^{out} because such the approximation can be used in the most of regions in the quasi-static situation ($\hat{R} \gg 1$). Thus, $(\nabla T)^2$ in the outer region may be approximated by

$$(\nabla T)_{out}^2 \simeq \frac{T_0^2 \alpha^2 p_0^2}{4C_p^2 a^2 \hat{r}^4}. \quad (30)$$

Of course, these assumptions cannot be used in general. In particular, near the edge $|x| = a$ the contribution is expected to be large. However, we believe that the evaluation under the simplified assumption may be useful as the first step of the analysis.

In the inner region, the integrand is independent of x and the integrated region may be approximated as a square domain $-a \leq x \leq a$ and $0 \leq y < 2R$. Thus, \dot{E}_{in} in (20) can be evaluated as follows: From

$$\int_0^{2\hat{R}} dt \left(1 - \frac{t}{\sqrt{1 + t^2}}\right)^2 = 2 + 4\hat{R} \left(1 - \sqrt{1 + \frac{1}{4\hat{R}^2}}\right) - \tan^{-1}(2\hat{R}) \simeq \frac{4 - \pi}{2} \quad (31)$$

with $\hat{R} \gg 1$, we obtain

$$\dot{E}_{in} \simeq -\frac{(4 - \pi)\kappa_T T_0 \alpha^2 F_{el}^2}{\pi^2 C_p^2 a^2}. \quad (32)$$

For the outer region, \dot{E}_{out} in (21) is

$$\dot{E}_{out} \simeq -\frac{\kappa_T T_0 \alpha^2 F_{el}^2}{4\pi C_p^2 a^2} \int d\hat{x} \int d\hat{y} \frac{1}{\hat{r}^4}. \quad (33)$$

The evaluation of the outer region is more complicated, because the domain

can not be approximated by a simple rectangular domain. For the evaluation, we neglect the deformation of shape of the compressed disk. Thus, the shape is approximated by a hemi-circle as in Fig. 10. It is convenient to introduce the polar coordinate (\hat{r}, θ) to evaluate (33). For a given angle θ between x axis and OQ in Fig. 10 \hat{r} is between $\hat{r}_{min} \equiv \overline{OP}/a$ and $\hat{r}_{max} = \overline{OQ}/a$. We also introduce θ_{min} which is the cutoff angle for θ . Taking into account $\hat{R} \gg 1$ we can evaluate

$$\hat{r}_{max} \simeq 2\hat{R} \sin \theta : \quad r_{min} \simeq \frac{1}{\cos \theta}. \quad (34)$$

Since these evaluations are approximate, we need to introduce the lower cutoff of θ_{min} by the consistency condition $\hat{r}_{max}(\theta_{min}) \geq \hat{r}_{min}(\theta_{min}) = 1$. Thus, $\theta_{min} \simeq a/2R$. The upper cutoff of θ is $\theta_{max} = \cot^{-1}(1/2\hat{R}) \simeq \pi/2 - 1/2\hat{R}$. Thus, the integral in (33) can be evaluated as

$$\begin{aligned} I &\equiv \int d\hat{x} \int d\hat{y} \frac{1}{\hat{r}^4} \simeq \int_{\theta_{min}}^{\theta_{max}} d\theta \int_{\hat{r}_{min}(\theta)}^{\hat{r}_{max}(\theta)} \frac{d\hat{r}}{\hat{r}^3} \\ &= -\frac{1}{8\hat{R}^2} \int_{\theta_{min}}^{\theta_{max}} \frac{d\theta}{\sin^2 \theta} + \frac{1}{2} \int_{\theta_{min}}^{\theta_{max}} d\theta \cos^2 \theta \simeq \frac{\pi}{8} - \frac{1}{2\hat{R}} \simeq \frac{\pi}{8}, \end{aligned} \quad (35)$$

where we use

$$\int_{\theta_{min}}^{\theta_{max}} \frac{d\theta}{\sin^2 \theta} = -\frac{1}{2\hat{R}} + \cot\left(\frac{1}{2\hat{R}}\right) \simeq 2\hat{R} + \frac{2}{3\hat{R}} \quad (36)$$

with $\cot \theta \simeq 1/\theta - \theta/3$ in the limit of $\theta \rightarrow 0$, and

$$\int_{\theta_{min}}^{\theta_{max}} d\theta \cos^2 \theta = \frac{\pi}{4} - \frac{1}{4\hat{R}}. \quad (37)$$

Substituting (35) into (33) we obtain

$$\dot{E}_{out} \simeq -\frac{\kappa_T T_0 \alpha^2 F_{el}^2}{32 C_p^2 a^2}. \quad (38)$$

From (32) and (38), the total dissipation rate $\dot{E} = \dot{E}_{in} + \dot{E}_{out}$ is given by

$$\dot{E} = -\gamma_0 \frac{\kappa_T T_0 Y \alpha^2 F_{el}}{C_p^2 (1 - \sigma^2) R} \quad (39)$$

where

$$\gamma_0 = \frac{\pi^2 + 128 - 32\pi}{256\pi^2}. \quad (40)$$

The result suggests that the dissipation rate by the thermal diffusion is dominant in quasi-static situations, because the force F_{el} appears in (39) exists even in the limit of zero impact velocity, while internal frictions considered in conventional quasi-static theory disappears in the limit of zero impact velocity.

This result, however, predicts a singular behavior of COR. In fact, the rough evaluation of the total energy loss E_{loss} by heat diffusion during the impact is proportional to the impact velocity v_i , while the definition of COR by E_{loss} is $E_{loss} = Mv_i^2(1 - e^2)/2$. Thus, COR may be singular for very small impact velocity. We need to consider another mechanism to remove such the singularity. We also need such the analysis for three dimensional situations where the stress field becomes simpler than that for two-dimensional cases (Hills et al. 1993).

6 Discussion

We investigate what happens in the disk above the critical velocity and find the existence of plastic deformation of the disk (Fig. 11(a)). Actually, there are no energy differences between two configurations in Fig. 11(b) which can occur after the strong compression during the impact but cannot be released after the impact is over. It is well known that plastic deformation causes the drop of the COR (Johnson, 1985).

6.1 Application of the Conventional Theory of Plastic Deformation to 2D Impacts

Following the description by Johnson (1985), let us explain the dimensional analysis of the two-dimensional plastic deformation. From two-dimensional Hertzian law (6) we evaluate $h \sim a^2/R$ (Johnson, 1985). The work for the compression of the disk W is $W = (1/2)Mv_i^2 \sim \int_0^{h^*} dh F_{el} \sim \int_0^{a^*} da a^3/R^2$, where M and v_i are the mass of the disk and the impact velocity, respectively. h^* and a^* are respectively the maximal compression and the maximal contact length. Here we neglect the logarithmic correction and unimportant numerical factors. Introducing the mean contact pressure during dynamical loading p_d which satisfies $p_d \sim F_{el}/a$, W can be evaluated by $W \sim F_{el}h^* \sim p_d(a^*)^3/R$. From $W \sim Mv_i^2$ we can express $a^* \sim (Mv_i^2 R/p_d)^{1/3}$.

Let us assume that the impact exceeds the yield pressure for the plastic deformation. In such the case, the deformation during rebound is frozen. Thus, the work in a rebound is $W' \sim F^*h^*$ where F^* is the maximal force during the impact. From $h^* \sim F^*/Y$ and $F^* \sim p_d a^*$ we evaluate $W' \sim (p_d a^*)^2/Y$.

Substituting the expression of a_0^* into the expression for W and W' we obtain the COR as

$$e^2 = \frac{v_r^2}{v_i^2} = \frac{W'}{W} \sim \frac{p_d^{4/3} R^{2/3}}{Y(Mv_i^2)^{1/3}}. \quad (41)$$

Thus, we expect the law $e \sim v_i^{-1/3}$ in the collision of a plastic deformed disk. The three dimensional version of evaluation which gives $e \sim v_i^{-1/4}$ agrees well with the experiment (Johnson, 1985).

6.2 Realistic Systems

The actual plastic deformation is more complicated than what we modeled in this paper. For example, in the actual contact area a central region of perfect contact is surrounded by an annulus of imperfect contact. In actual situations, it is not easy to obtain a pure normal collision, because the rotation of disks is difficult to be suppressed and the wall is not perfectly flat. Thus, a little deviation of the collision angle causes the tangential stress in collisions. In the existence of tangential stress, we need to consider the effect of imperfect contact or partial slip in the outer region to get finite force at the corner of contact area.

We also note that the actual materials are not uniform. They contain a lot of microcracks, and amorphous structure locally. Such the imperfection of the materials causes the local achievement of the yield of plastic deformation. Thus, the plastic deformation also occurs localized in contrast to the macroscopic deformation in Fig.11.

Our finding is, however, something new, because (i) the decrease of COR is

excited by the temperature and (ii) COR decreases more rapidly like $e \sim v_i^{-1.2}$ than that for the conventional plastic deformation $e \sim v_i^{-1/3}$ in (41). The mechanism how to occur the plastic deformation is not clear at present including the linear law in Fig. 9.

For future refinement of our model to describe plastic deformation, we need to introduce (i) the initial cracks, (ii) local deformation of lattices at the initial condition, (iii) the yield of local plastic deformation or non-Hookian effects of springs, and (iv) porosity distribution at the initial condition except for the introduction of the heat diffusion effects as introduced in section 5. Of course, to compare the simulation with experiments, we have to simulate the model in three dimensional situations.

7 Conclusion

We have numerically studied the impact of a two dimensional elastic disk with the wall with the aid of model A and model B. The result can be summarized as (i) The coefficient of restitution (COR) decreases with the impact velocity. (ii) The result of our simulation is not consistent with the result of the two-dimensional quasi-static theory. For large impact velocity, there is hysteresis in the deformation of the center of mass. For small velocity, there remains the inelastic force even at $\dot{h} = 0$. (iii) The effect of heat diffusion may be important for the small impact velocity. (iv) There are drastic effects of temperature in both small and large impact velocity. (v) In particular, for large impact velocity of model A, we have found the abrupt drop of COR above the critical impact velocity by the plastic deformation. The critical velocity of the plastic deformation seems to obey a simple linear function of temperature.

We believe that this preliminary report is meaningful to recognize that physicists have poor understanding of such the fundamental process of elementary mechanics. We hope that this paper will invite a lot of interest in the impact from various view points. We, at least, have a plan to study three dimensional impacts to clarify the relation among the microscopic simulation, experiments and the quasi-static elastic theory.

Appendix

A Langevin Approach to the Quasi-Static Theory

In this Appendix let us introduce the derivation of quasi-static theory by Morgado and Oppenheim (1997). The characteristics of their derivation is to introduce 'thermal deformation' explicitly to assist the elastic deformation. Although they do not mention what the thermal deformation is, it is the complex combination of inelastic scattering of phonons, electrons, sound radiation into the air and any other mechanism which cannot be regarded as the elastic deformation. In this Appendix we introduce a simplified version of the derivation of Langevin equation instead of using the original argument (Morgado & Oppenheim, 1997). Note that the argument in this Appendix is restricted to one in three dimensional systems.

Thus, the position \mathbf{d}_i of i -th. atom can be written as $\mathbf{d}_i = \mathbf{R}_i + \mathbf{u}_i + \boldsymbol{\rho}_i$, where \mathbf{R}_i , \mathbf{u}_i , and $\boldsymbol{\rho}_i$ are respectively the equilibrium position of the atom i , the elastic deformation and the 'thermal' deformation. Here the terminology

of 'thermal' deformation means that the deformation cannot be controlled or the origin has not been specified from macroscopic point of view. Such the 'thermal' deformations may be regarded as a not important variables which can be treated as random variables. Let us introduce $\boldsymbol{\xi}_i = \mathbf{d}_i - \mathbf{R}_i$. In the local rule in this Appendix, suffices i, j represent atoms, and the Greek suffices such as α, β are components. In addition, we adopt Einstein's rule for suffices where the duplicated suffices mean the summation as $a_\alpha b_\alpha \equiv \sum_\alpha a_\alpha b_\alpha$. For small deformation, $\boldsymbol{\xi}_i$ can be written as

$$\boldsymbol{\xi}_i \simeq \mathbf{R}_i \cdot \frac{\partial}{\partial \mathbf{x}_i} \mathbf{u}(\mathbf{R}_i) + \boldsymbol{\rho}_i. \quad (\text{A.1})$$

The potential among atoms can be approximated by a harmonic one near its equilibrium position. Thus, the harmonic potential for isotropic systems is given by

$$U_0 = \frac{\kappa}{2} \sum_i \boldsymbol{\xi}_i^2. \quad (\text{A.2})$$

Note that the original paper(Morgado & Oppenheim, 1997) does not assume isotropic form of U_0 . Then U_0 is replaced by a second order tensor. Substituting (A.1) into (A.2), eq.(A.2) becomes the combination of three terms:

$$U_0 = U_{el} + U_\phi + U_H \quad (\text{A.3})$$

The first term of the right hand side of (A.3) is the elastic energy for the deformation which can be written as

$$U_{el} = \sum_i \left\{ \frac{\lambda}{2} u_{\alpha\alpha}(\mathbf{R}_i) u_{\beta\beta}(\mathbf{R}_i) + \mu u_{\alpha\beta}(\mathbf{R}_i) u_{\alpha\beta}(\mathbf{R}_i) \right\}, \quad (\text{A.4})$$

where $\kappa R_\alpha R_\beta = \mu \delta_{\alpha\beta} + \frac{\lambda}{2} \delta_{\alpha\gamma} \delta_{\gamma\beta}$ Note that in the original paper (Morgado &

Oppenheim, 1997), the coefficient of $u_{\alpha\beta}u_{\gamma\delta}$ becomes a fourth-order tensor. U_ϕ also includes a constant which is represented by a second-order tensor.

Here, λ and μ are Lamé's elastic coefficients. The second term of right hand side of (A.3) is given by

$$U_\phi = \kappa \sum_{i,j} R_{i\alpha} u_{\alpha\nu} \rho_{j\nu},$$

which expresses the coupling between the elastic deformation and the thermal deformation. The third term of (A.3), $U_H = \frac{\kappa}{2} \sum_{i,j} \rho_{i\alpha} \rho_{j\alpha}$, is the energy of the thermal deformation. The contribution of this term is in general smaller than other terms.

The collision of two elastic bodies consists of materials 1 and 2. The energy is the simple summation of the contribution of two materials. Let the center of mass of i -th particle $\mathbf{r}^{(i)}$ ($i = 1, 2$). The interaction during collision appears if $r_{12} = |\mathbf{r}^{(1)} - \mathbf{r}^{(2)}| < 2R$.

Morgado and Oppenheim (1997) assume that the slow mode, the motion of the center of mass, can be written by the solution of the Langevin equation. In the Langevin equation, the elastic force is regarded as a systematic force, while the force $-\nabla U_\phi$ plays a role of the fluctuating force. As in the general framework of the fluctuation-dissipation theorem, the friction coefficient $\zeta(r_{12})$ in the Langevin equation is determined by the time correlation function of the fluctuating force as

$$\zeta(r_{12}) = \int_0^\infty d\tau \langle \nabla U_\phi \nabla U_\phi(\tau) \rangle. \quad (\text{A.5})$$

Here $\nabla U_\phi(\tau)$ is retarded one of ∇U_ϕ by time τ . Thus, we can write

$$\zeta(r_{12}) = \kappa^2 \sum_{k=1}^2 \sum_{i,j} R_\alpha^{(k)} R_\beta^{(k)} (\nabla_{12} u_{\beta\gamma}^{(k)}) (\nabla_{12} u_{\alpha\delta}^{(k)}) \int_0^\infty d\tau \langle \rho_{i\delta}^{(k)} \rho_{j\gamma}^{(k)}(\tau) \rangle, \quad (\text{A.6})$$

where $\nabla_{12} = \nabla_{\mathbf{r}_{12}}$ and the upper suffix (k) represents the particles 1,2. Here, ρ_i can be regarded as the thermal fluctuation as

$$\langle \rho_{i\alpha}^{(k)} \rho_{j\beta}^{(k)}(\tau) \rangle = \frac{T_v}{\kappa} T \delta_{ij} \delta_{\alpha\beta} \delta(\tau). \quad (\text{A.7})$$

Thus, we obtain

$$\zeta(r_{12}) = T \frac{T_v}{\kappa} \sum_{k=1}^2 R_\alpha^{(k)} R_\beta^{(k)} (\nabla_{12} u_{\beta\gamma}^{(k)}) (\nabla_{12} u_{\alpha\gamma}^{(k)}). \quad (\text{A.8})$$

Let us recall that Kramer's equation for many-body systems

$$\begin{aligned} \frac{\partial P(X_t, t)}{\partial t} = & \left[\left(- \sum_{i=1}^2 \frac{\mathbf{p}_i}{M} \cdot \nabla_{\mathbf{r}_i} + \sum_{i=1}^2 \nabla_{\mathbf{r}_i} U_{el} \nabla_{\mathbf{p}_i} \right) \right] P(X_t, t) \\ & + \left[\frac{1}{2} \sum_{j(\neq k)=1}^2 \zeta_{12} \hat{\mathbf{r}}_{jk} \hat{\mathbf{r}}_{jk} : \nabla_{\mathbf{p}_{kj}} \left(\beta \frac{\mathbf{p}_{kj}}{M} + \nabla_{\mathbf{p}_{kj}} \right) \right] P(X_t, t) \end{aligned} \quad (\text{A.9})$$

is equivalent to the Langevin equation, where $\beta = 1/T$, $X_t = \{\mathbf{p}_i(t), \mathbf{r}_i(t)\}$ ($i = 1, 2$), $\zeta_{12} = \zeta(r_{12})$, $\mathbf{p}_{kj} = \mathbf{p}_j - \mathbf{p}_k$, $\nabla_{\mathbf{p}_{kj}} = \nabla_{\mathbf{p}_j} - \nabla_{\mathbf{p}_k}$. $\hat{\mathbf{r}}_{jk}$ is the unit vector from the center of j th. particle to the center of k -th. particle. Here we introduce the average $\langle B \rangle_t$ as $\langle B \rangle_t \equiv \int dX_t B P(X_t, t)$ for any variable B . Note that we have the relation

$$\frac{d}{dt} \langle B \rangle_t = \int dX_t B \frac{\partial P}{\partial t}. \quad (\text{A.10})$$

Introducing the relative coordinate $\mathbf{r}_{12} = \mathbf{r}_2 - \mathbf{r}_1$ approximating that the potential U_0 is approximated by U_{el} we obtain

$$\begin{aligned}
\langle \dot{\mathbf{p}}_{12} \rangle_t &= - \int dX_t P(X_t, t) (\nabla_{\mathbf{r}_1} U_{el} - \nabla_{\mathbf{r}_2} U_{el}) - \frac{\beta}{M} \int dX_t \zeta_{12} \hat{\mathbf{r}}_1 \hat{\mathbf{r}}_2 \cdot \mathbf{p}_{12} P(X_t, t) \\
&= \langle \mathbf{F}_{el} \rangle_t - \frac{\beta}{M} \langle \zeta_{12} \hat{\mathbf{r}}_{12} \hat{\mathbf{r}}_{12} \cdot \mathbf{p}_{12} \rangle_t.
\end{aligned} \tag{A.11}$$

Note the contribution of the linear momentum disappears from the integral by parts. The elastic force $\langle \mathbf{F}_{el} \rangle = -\hat{\mathbf{r}}_{12} U'_{el}(h)$ is nothing but the Hertzian contact force, and $U_{el} = \frac{k_h}{2} h^{5/2}$. Thus, the time evolution of the macroscopic deformation h (h satisfies $h = 2R - r_{12}$.) is given by

$$\frac{M}{2} \ddot{h} = -\frac{5}{4} k_h h^{3/2} - \frac{\beta \zeta(h)}{M} \dot{h}. \tag{A.12}$$

Therefore, to determine the dissipation is reduced to determination of the friction constant $\zeta(h)$.

Unfortunately, it is impossible to obtain the exact form of $\zeta(h)$, because ζ is determined from the complicated relations between the elastic deformation and the thermal deformation. However, from the consideration of power counting of h it is not difficult to deduce how $\zeta(h)$ depends on h . In fact, it is easy to show the scaling $u_z(\mathbf{x}) \rightarrow u_z(\sqrt{\alpha}\mathbf{x}) = \alpha u_z(\mathbf{x})$ in the Hertzian contact theory. Similarly we have $u_{\alpha\beta}(\mathbf{x}) \rightarrow u_{\alpha\beta}(\sqrt{\alpha}\mathbf{x}) = \sqrt{\alpha} u_{\alpha\beta}(\mathbf{x})$ and $\partial u_{\alpha\beta}(\mathbf{x})/\partial h \rightarrow \partial u_{\alpha\beta}(\sqrt{\alpha}\mathbf{x})/\alpha \partial h = 1/\sqrt{\alpha} (\partial u_{\alpha\beta}(\mathbf{x})/\partial h)$. From the comparison between the elastic energy (A.4) and $\zeta(h)$ in (A.8), it is easy to understand that the key point is how $u_{\alpha\beta}$ and $\partial u_{\alpha\beta}/\partial h$ are scaled by α . From the discussion here the elastic energy is scaled as $\alpha^{5/2}$, and thus $\zeta(h)$ is scaled as $\alpha^{1/2}$. Thus, we finally obtain

$$\zeta(h) = \frac{5}{2} k' h^{1/2} \tag{A.13}$$

and

$$\frac{M}{2}\ddot{h} = -\frac{5}{4}k_h h^{3/2} - \frac{5}{2}k''\dot{h}, \quad (\text{A.14})$$

where $k'' = \beta k'/M$ and k' cannot be determined from this argument. This result agrees with the result by the viscous stress tensor (Kuwabara & Kono, 1987; Brilliantov et al., 1996).

Note that the derivation is quite different from the previous one assumed the existence of viscous tensor. Both of derivation assumed that the temperature field is uniform, but this assumption is not correct in general. As discussed in the text, the rise of temperature is directly related to the compression. Since the compression is not uniform, the rise of temperature is not uniform.

Two-dimensional quasi-static theory in eq. (8) can be derived by a parallel argument introduced in this Appendix.

Acknowledgment

We appreciate S. Sasa, S. Takesue, Y.Oono and H. Tasaki for their valuable comments. One of the authors(HK) thanks S. Wada, K. Ichiki, A. Awazu, and M. Isobe for stimulative discussions.

Notation¹

¹ In this paper, we analyze two dimensional systems. As a result many of quantities have different dimensions from those for usual three dimensional ones. We also note that we do not introduce Boltzmann's constant in the calculation. Thus, T has the same dimension with E , and the entropy becomes dimensionless.

a_0	coefficient of a wall potential, 1/m
a	contact radius, m
A, A_h	constants, s
c	one dimensional sound velocity, m/s
c_l	sound velocity of the longitudinal mode, m/s
C_p	heat capacity at constant pressure, dimensionless
c_t	sound velocity of the tangential mode, m/s
d_0	lattice constant, m
e	coefficient of restitution, dimensionless
\mathbf{e}_y	the unit vector of y direction.
E	energy (2D), J/m
E_{loss}	energy loss during an impact (2D), J/m
\dot{E}	the dissipation rate (2D), J/m·s
\dot{E}_{in}	the dissipation rate in the internal region (2D), J/m·s
\dot{E}_{out}	the dissipation rate in the outer region (2D), J/m·s
F_{el}	2D elastic force, N/m
F_{tot}	2D total force, N/m

g	an external field, dimensionless
h	macroscopic deformation, m
H	2D Hamiltonian, J/m
$J_n(x)$	n-th order Bessel function
k_h	the constant in eq.(3)
K	2D bulk modulus, N/m
K_{ad}	2D bulk modulus in the adiabatic process, N/m
m	mass of a mass point (2D), kg/m
M	mass of an elastic disk (2D), kg/m
M_0	mass of a sphere, kg
$P_{n,l}$	canonical momentum (2D), kg/s
p_0	the constant in eq.(23)
$Q_{n,l}$	canonical coordinate, m
R	radius of the disk, m
\hat{R}	dimensionless radius (R/a)
\mathbf{r}_i	position of mass point
\hat{r}_{max}	maximum distance from origin, dimensionless

\hat{r}_{min}	minimum distance from origin, dimensionless
\hat{r}	distance from origin, dimensionless
s	defined in eq.(22)
S_0	dimensionless entropy,
t	time, s
T	temperature (2D), J/m
T_0	temperature without deformation, J
u_i	displacement field, m
u_{ij}	strain tensor, dimensionless
V_0	coefficient of wall potential, J/m
v_i	impact velocity, m/s
v_r	rebound velocity, m/s
v_{th}	thermal velocity, m/s
\hat{x}	dimensionless x coordinate of the position (x/a)
Y	Young's modulus (2D), N/m
Y_0	Young's modulus (3D), N/m ²
y_0	position of center of mass, m

y_p	y coordinate of r_p , m
$y(\phi, t)$	the shape of an elastic disk, m
\hat{y}	dimensionless y coordinate of the position (y/a)

Greek letters

α	thermal expansion rate (2D), m/N
β	$1/T$
η_i	viscous constant (2D), N·s/m
γ_0	the dimensionless constant in eq.(40)
κ	spring constant, N/m
κ_T	thermal conductivity (2D), 1/s
μ	shear modulus (2D), N/m
ρ	density (2D), kg/m ²
σ	Poisson's ratio, dimensionless
$\sigma_{ij}^{(el)}$	2-dimensional static stress tensor
σ_{ii}^{in}	stress tensor in the inner region

σ_{ii}^{out} stress tensor in the outer region

Δt time step for simulation, s

τ contact time, s

References

Aspelmeier, T., Giese, G., & Zippelius, A. (1998). Cooling dynamics of a dilute gas of inelastic rods: A many particle simulation. *Phys. Rev. E*, 57, 857-865

Basile, A. G., & Dumont, R. S. (2000). Coefficient of restitution for one-dimensional harmonic solids. *Phys. Rev. E*, 61, 2015-2023.

Bridges, F. G., Hatzes, A., & Lin, D.N.C. (1984). Structure, Stability and evolution of Saturn's rings. *Nature*, 309, 333-335.

Brilliantov, N., Spahn, F., Hertzsch, J.-M. & Pöschel, T. (1996). Model for collisions in granular gases. *Phys. Rev. E*, 53, 5382-5392.

Cundall, P. A., & Strack, O. D. L. (1979). A discrete numerical model for granular assemblies. *Géotechnique*, 29, 47-65.

de Gennes, P. G. (1999). Granular matter: a tentative view. *ibid*, S367-S382 and references therein.

Gerl, F., & Zippelius, A. (1999). Coefficient of restitution for elastic disks. *Phys. Rev. E*, 59, 2361-2372.

- Giese,G., & Zippelius,A. (1996). Collision properties of one-dimensional granular particles with internal degrees of freedom. *Phys. Rev. E*, 54, 4828-4837
- Goldsmith,W. (1960). *Impact : The Theory and Physical Behavior of Colliding Solids* London:Edward Arnold Publ.
- Hayakawa,H., & Kuninaka,H. (2001a). *Simulation of the Impact of Two-dimensional Elastic Disks* , in the Proceedings of the Nineth Nisshin Engineering Particle Technology International Symposium on 'Solids Flow Mechanism and Their Applications', 82-95.
- Hayakawa, H., & Kuninaka, H. (2001b). *Coefficient of restitution of elastic disk*, the Proceedings of Powders and Grains 2001 (edited by Y. Kishino), 561-564, Rotterdam:A. A. Balkema Publ.
- Hertz,H. (1882a). Über die Berührung fester elastische Körper. *J. Reine Angew. Math.*, 92, 156-171.
- Hills,D. A., Nowell,D., & Sackfield,A. (1993). *Mechanics of Elastic Contacts* Oxford:Butterworth-Heinemann.
- Hoover,W. G. (1991). *Computational Statistical Mechanics*. Amsterdam:Elsevier Science Publishers B. V.
- Johnson,K. L. (1985). *Contact Mechanics*. Cambridge: Cambridge University Press.
- Kadanoff,L. P. (1999). Built upon sand: Theoretical ideas inspired by granular flows. *Rev. Mod. Phys.*, 71, 435-444.
- Kuninaka,H., & Hayakawa,H. (2001). The impact of two-dimensional elas-

- tic disk, *J. Phys. Soc. Jpn.*, 70, 2220-2221 .
- Kuwabara,G. & Kono,K. (1987). Restitution Coefficient in a Collision between Two Spheres. *Jpn. J. Appl. Phys.*, 26, 1230-1233.
- Labous,L., Rosato,A.D., & Dave,R. N. (1997). Measurements of collisional properties of spheres using high-speed video analysis. *Phys. Rev. E*, 56, 5717-5725.
- Landau,L. D.,& Lifshitz,E. M. (1960). *Theory of Elasticity*(2nd English ed.). New York:Pergamon.
- Love,A. E. H. (1927). *A Treatise on the Mathematical Theory of Elasticity*. Cambridge:Cambridge Univ. Press.
- Mindlin,R. D. (1949). Compliance of Elastic Bodies in Contact. *J. Appl. Mech. Trans. ASME*, 16, 259 See also ref.7.
- Morgado,W. A., & Oppenheim,I. (1997). Energy dissipation for quasielastic granular particle collisions. *Phys. Rev. E*, 55, 1940-1945.
- Newton,I. (1962). *Philosophiae naturalis Principia mathematica*. London:W. Dawason and Sons. The original one has been published in 1687
- Ramírez,R., Pöschel,T., Brilliantov,N. & Schwager,T. (1999). Coefficient of restitution of colliding viscoelastic spheres. *Phys. Rev. E*, 60, 4465-4472 .
- Schwager,T., & Pöschel,T. (1998). Coefficient of normal restitution of viscous particles and cooling rate of granular gases. *Phys. Rev. E*, 57, 650- 654.
- Sondergaard,R., Chaney,K., & Brennen,C. E. (1990). Measurements of Solid Spheres Bouncing off Flat Plates. *Transaction of the ASME, Journal of*

Applied Mechanics, 57, 694-699.

Supulver, K. D., Bridges, F. G., & Lin, D. N. C. (1995). The Coefficient of Restitution of Ice Particles in Glancing Collisions: Experimental Results for Unfrosted Surfaces. *ICARUS*, 113, 188-199.

Figure 1: A schematic figure of a disk used in model A.

Figure 2: Coefficient of restitution for normal collision of the Model A and Model B as a function of impact velocity, where $c = \sqrt{Y/\rho}$ with Young's modulus Y and the density ρ . 437 and 1189 modes are chosen for model B. The error bar in model A represents the standard deviation of the data as a function of the initial orientation θ .

Figure 3: The comparison of the Hertzian force in eq.(6) with our simulation at $v_i = 0.01c$ (a) and $v_i = 0.001c$ (b) at $T = 0$ in model B. F_{tot} is the total force originated from the interaction with a wall.

Figure 4: The time evolution of the center of mass of the elastic disk under the compression by $g = 0.01c^2/R$ (model B with $N=437$). Here the dimensionless time is measured by R/c and the position of C.M. (center of mass) is measured by the diameter of the disk ($2R$). Simulation is performed at the finite temperature $T = 10^{-8}Mc^2$ and is averaged over 20 independent samples which start from initial condition satisfying the Gibbs distribution.

Figure 5: The plot of contact time versus the impact velocity (model A). R represents the radius of the disk, in which $R = 40,60,70$ and 80 correspond to the number of mass points 5815, 13057, 17761 and 23233, respectively. The dash-dotted line is fitting curve based on the quasi-static theory. Here the line represents the fit of $\tau c/R$ as $3.21758\sqrt{\ln(4c/v_i)} \sim \pi\sqrt{\ln(4c/v_i)}$.

Figure 6: The average shift of COR at finite temperature $T = 10^{-8}Mc^2$ as a function of the impact velocity in model B with $N = 437$. The dotted line indicates one at $e(T) = e(0)$.

Figure 7: The standard deviation of COR $\sigma = \sqrt{\langle (e - \langle e \rangle)^2 \rangle}$ at $T =$

$10^{-8}Mc^2$ as a function of the impact velocity v_i via model B with $N = 437$.

Figure 8: The relation between the coefficient of restitution and the impact velocity rescaled by the critical velocity for each temperature. Curves are plotted in the log-log scale. The temperature is scaled by $T_0 = mc^2$ with the mass of the mass points m . Note that the error bars are plotted only in the case $T/T_0 = 0.03$ but are the same order even at other T (model A).

Figure 9: The plot of the initial temperature and the critical velocity causing the plastic deformation. $v_{cr}/c = a(T/T_0) + b$ is the fitting curve line from the data between $T/T_0 = 0.02$ and 0.05 (model A).

Figure 10: The configuration of a compressed disk. The origin is O . The angle between OP and x axis is θ . The inner region is inside two vertical dashed line, while the outer region is outside the central region. The length of OS is equal to a . The radius of (undeformed) disk is R .

Figure 11: (a) Plastic deformation of model A with $v_i = 0.22c$ at $T = 0.03mc^2$. The solid circle represents the initial circle. The points in a circle are positions of the mass points after the collision. The deformation is asymmetric because of the velocity distribution at the initial stage. (b) All the mass points of the disk initially consist of a triangular lattice. When the deformation occurs, it is possible that the configuration of mass points (points in figure) locally change like this figure. Note that these two configurations are energetically equivalent.

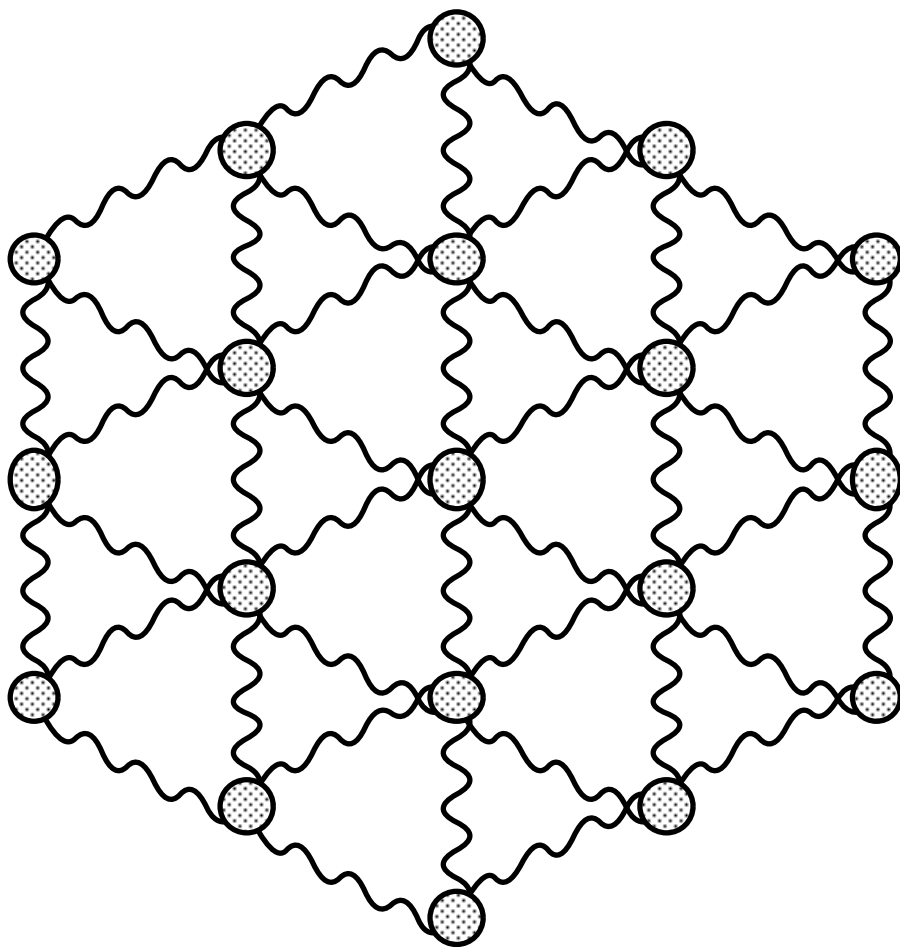


Fig. 1. authors: Hisao Hayakawa & Hiroto Kuninaka

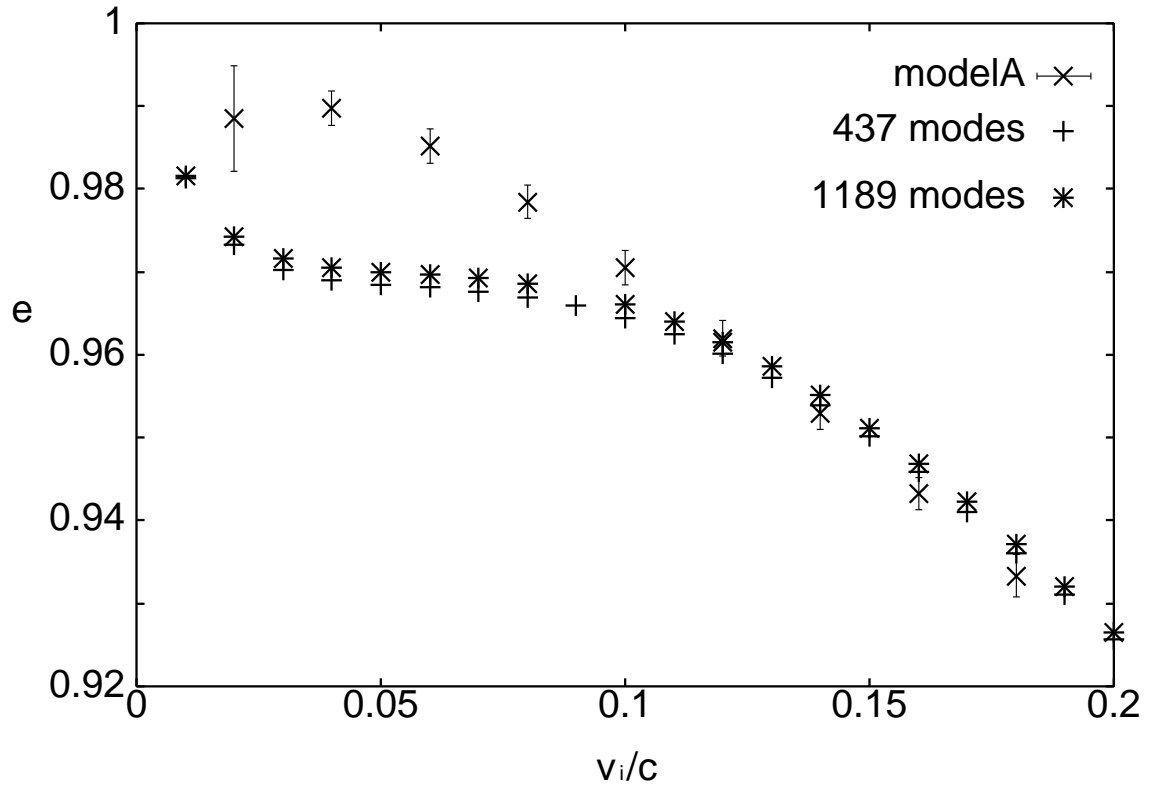
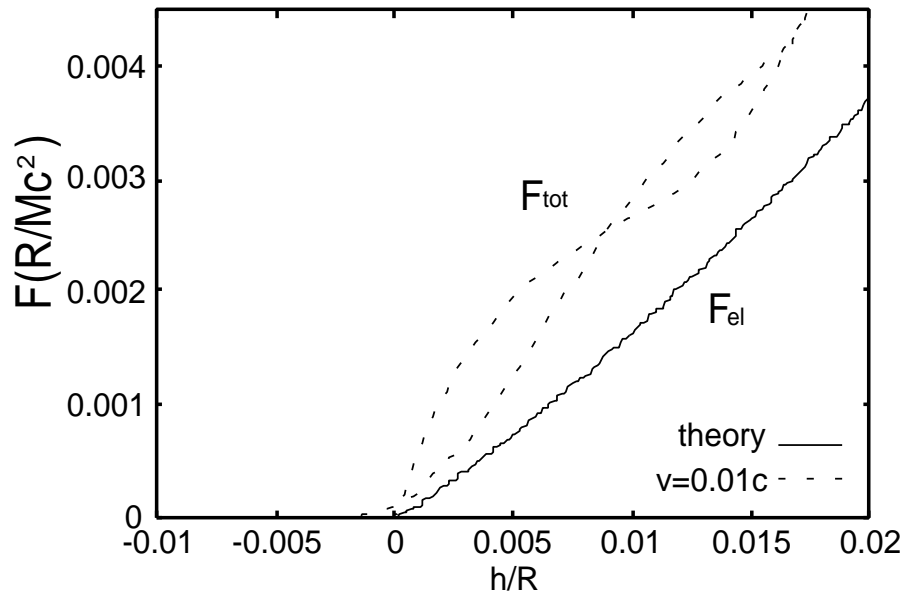
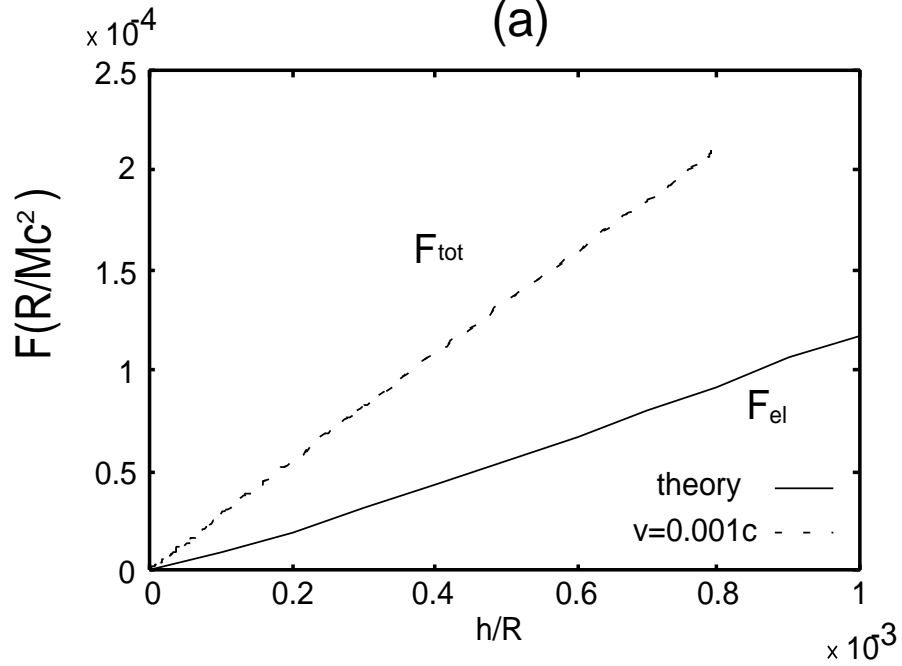


Fig. 2. authors: Hisao Hayakawa & Hiroto Kuninaka



(a)



(b)

Fig. 3. authors: Hisao Hayakawa & Hiroto Kuninaka

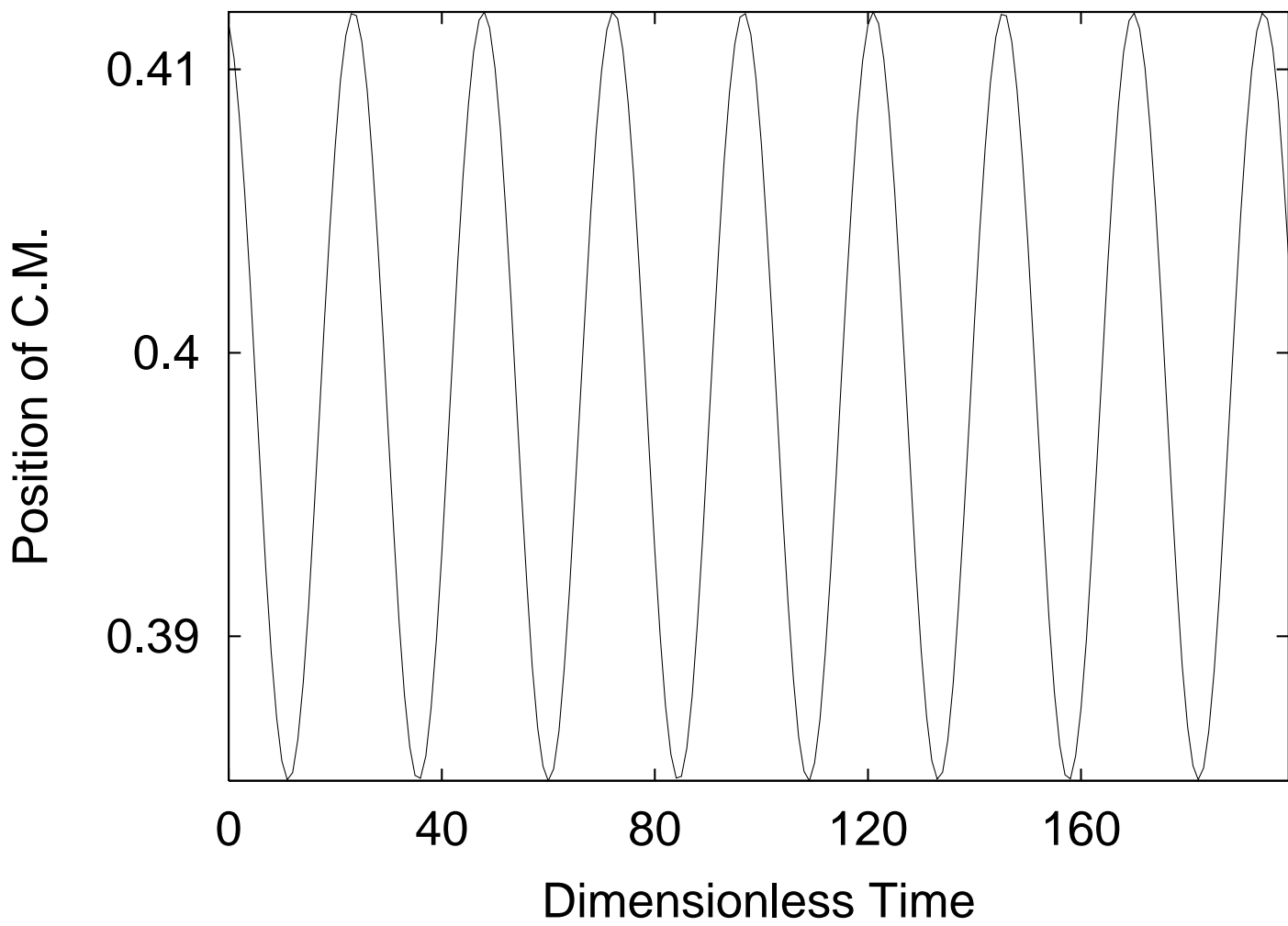


Fig. 4. authors: Hisao Hayakawa & Hiroto Kuninaka

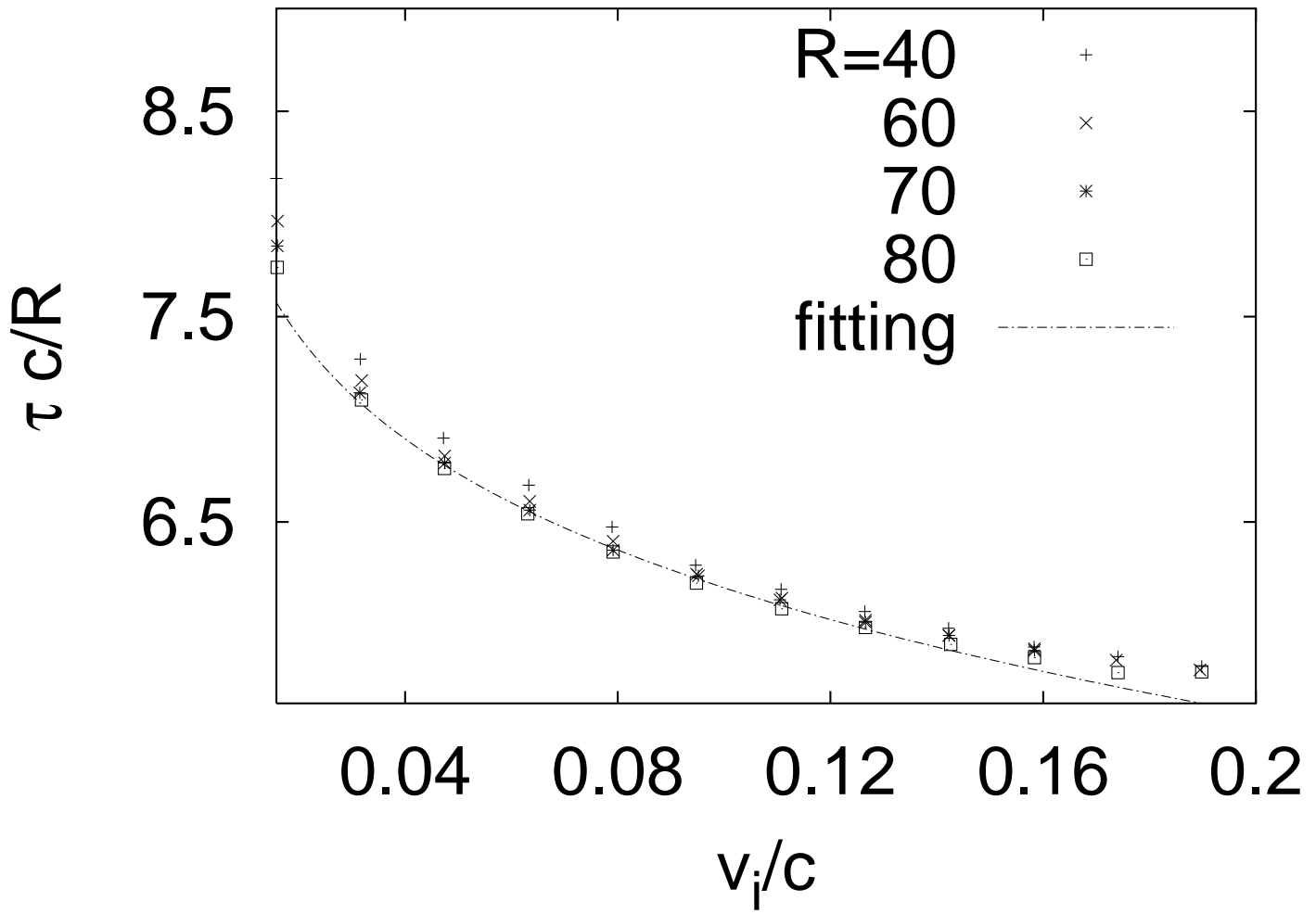


Fig. 5. authors: Hisao Hayakawa & Hiroto Kuninaka

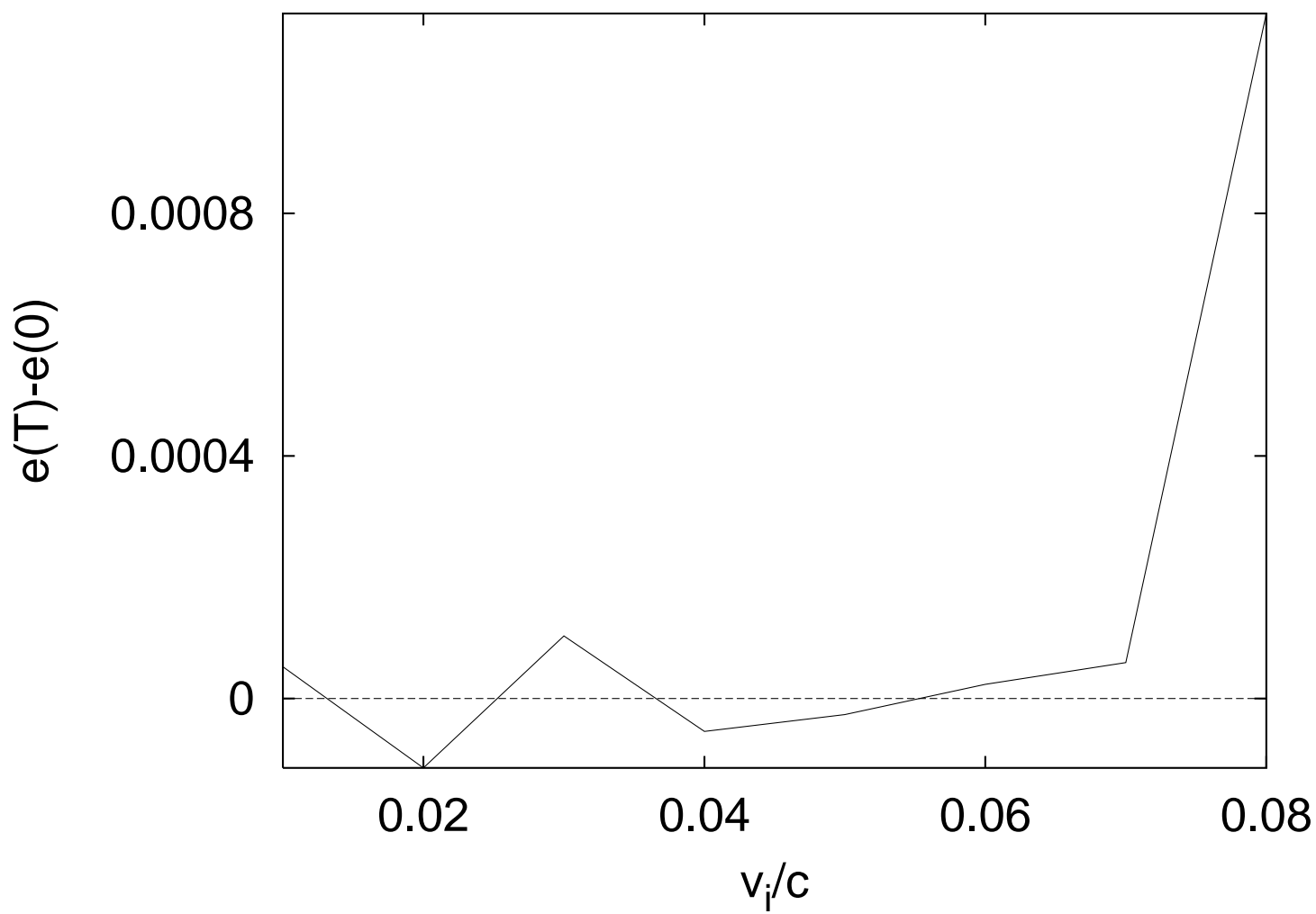


Fig. 6. authors: Hisao Hayakawa & Hiroto Kuninaka

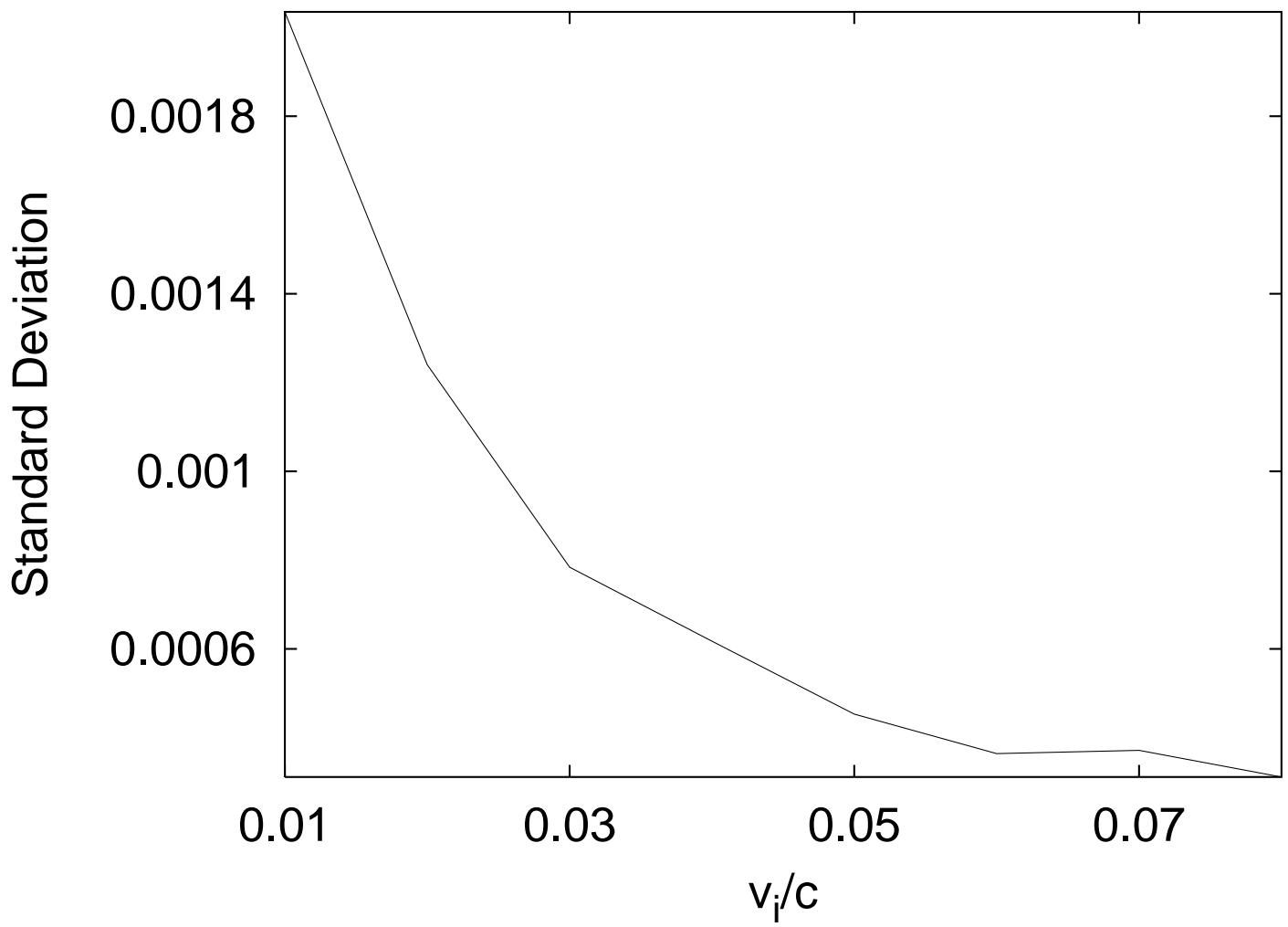


Fig. 7. authors: Hisao Hayakawa & Hiroto Kuninaka

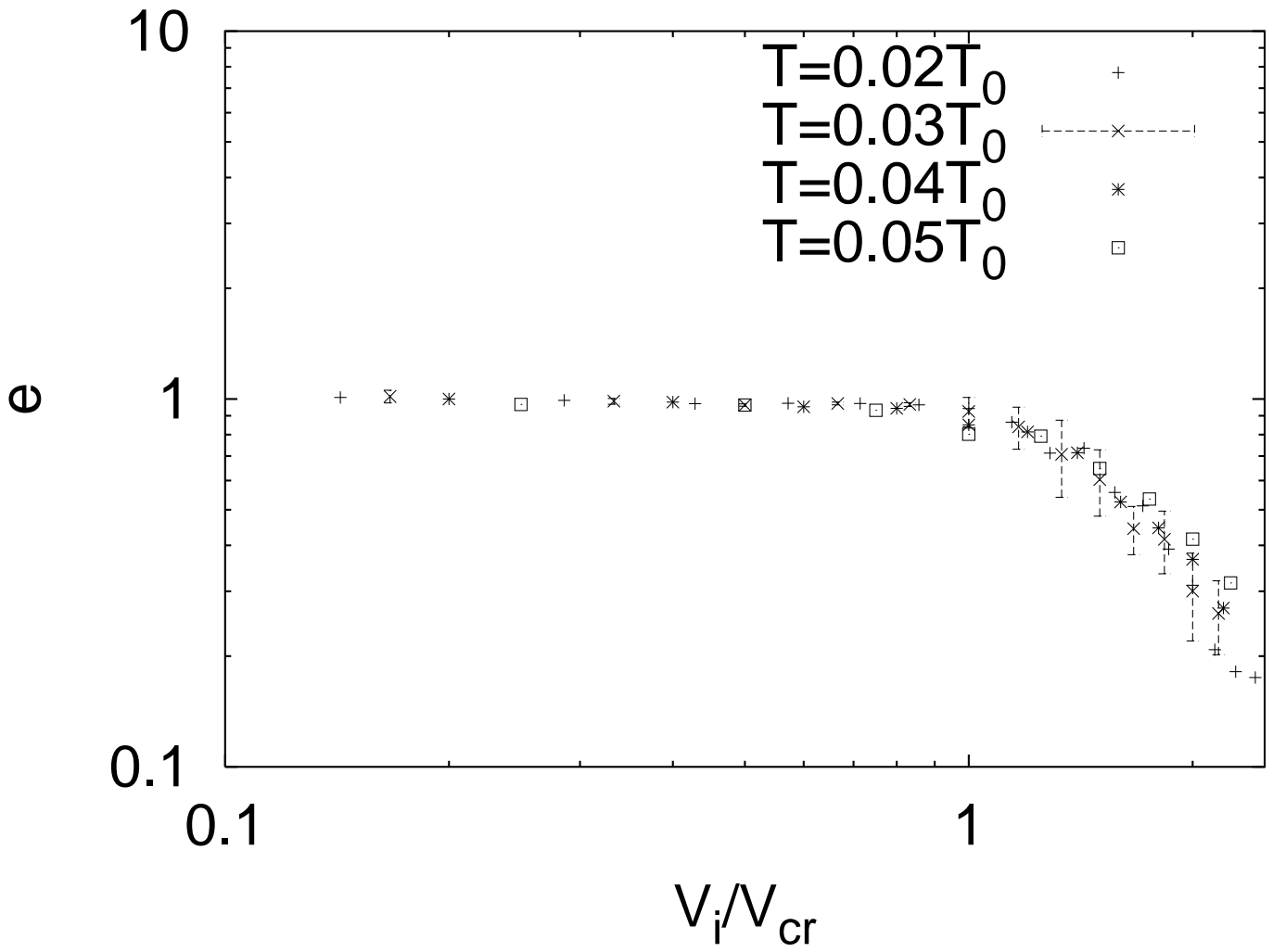


Fig. 8. authors: Hisao Hayakawa & Hiroto Kuninaka

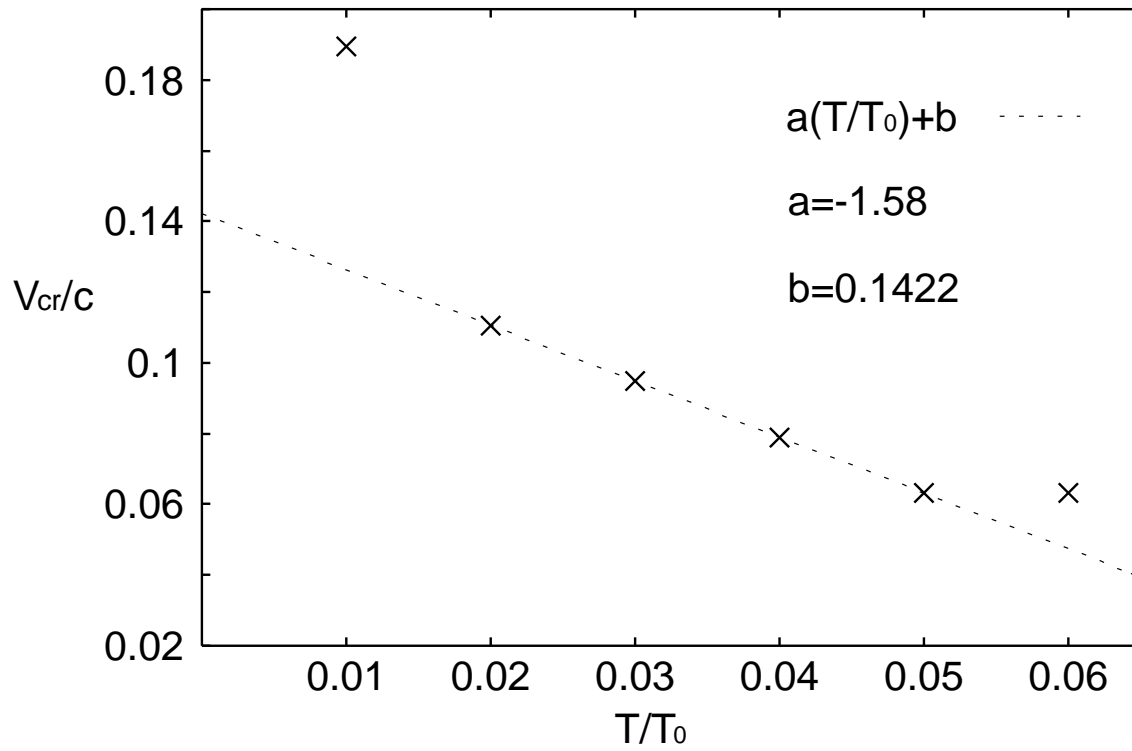


Fig. 9. authors: Hisao Hayakawa & Hiroto Kuninaka

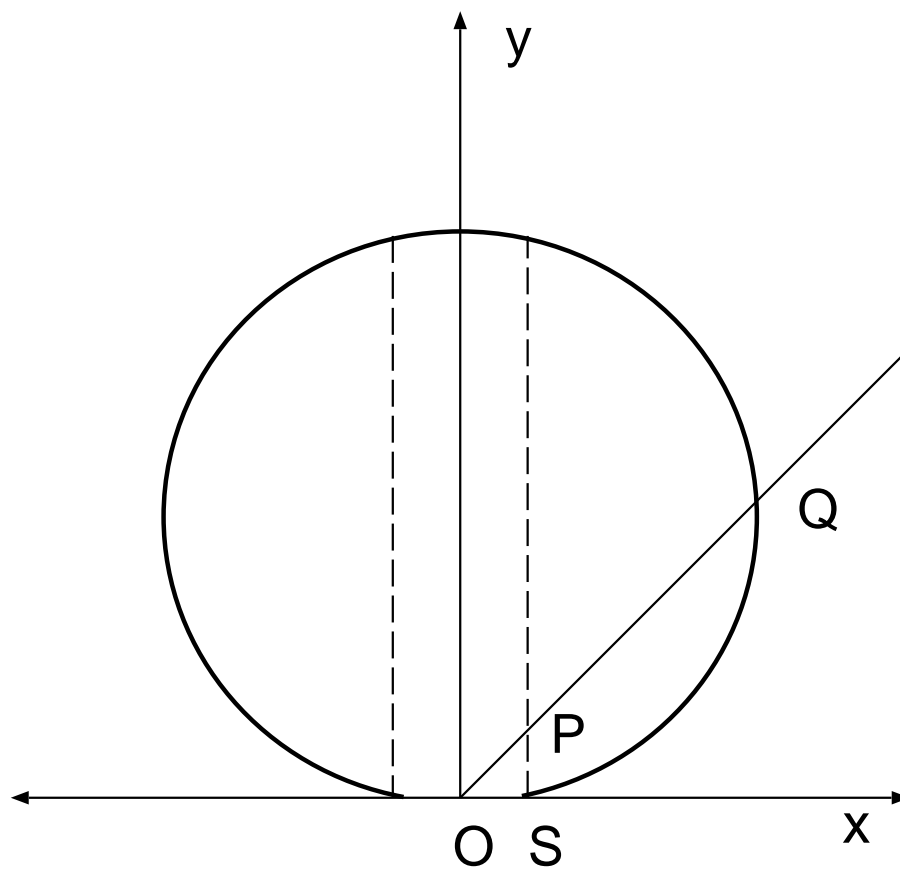
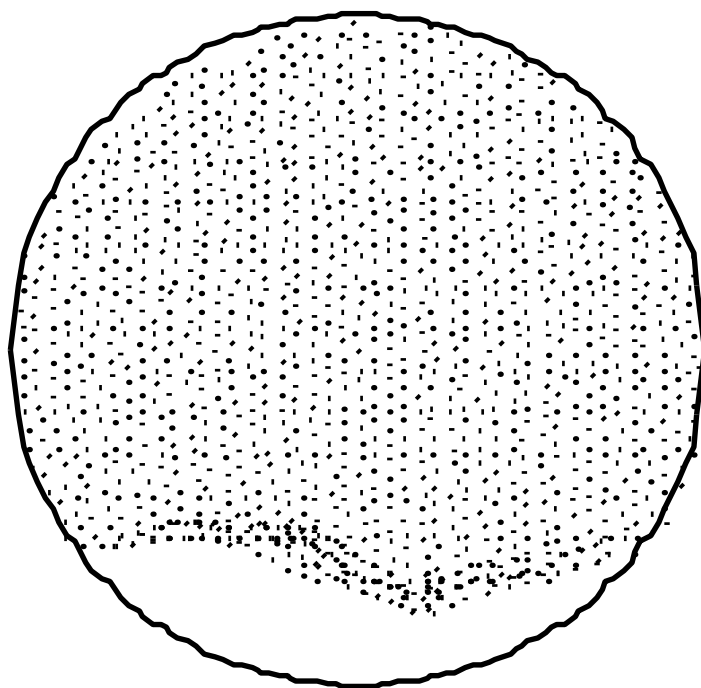


Fig. 10. authors: Hisao Hayakawa & Hiroto Kuninaka

(a)



(b)

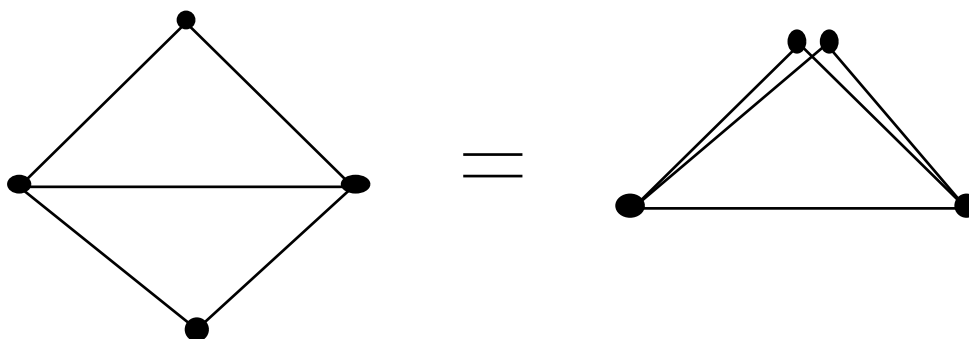


Fig. 11. authors: Hisao Hayakawa & Hiroto Kuninaka